Buffer-Aided Adaptive Wireless Powered Communication Network With Finite Energy Storage and Data Buffer

Xiaolong Lan, Qingchun Chen, *Senior Member, IEEE*, Lin Cai, *Senior Member, IEEE*, and Lisheng Fan

***Abstract*— In this paper, the access point (AP) in a wireless network is assumed to provide energy supply via wireless energy transfer to multiple terminals in the downlink, and all the terminals use the harvested energy to transmit their collected data to the AP in the uplink in a time division multiple access (TDMA) manner. Each terminal is provisioned with a finite energy storage and a finite data buffer to store the harvested energy and to buffer the arrived data traffic, respectively. Due to the limited data buffer and energy storage size, there might be data loss due to either data buffer overflow or energy storage depletion. Firstly, we aim at maximizing the long-term weighted sum-rate through energy beamforming vector design, power allocations, rate control, time allocations, and transmission mode selection subject to average transmit power, peak transmit power, data loss ratio requirements, practical data buffer as well as energy storage constraints. Secondly, the weighted max-min scheduling scheme is proposed to guarantee the fair access requirement by multiple terminals. Numerical analyses are presented to show that, the proposed adaptive design can substantially improve the average achievable rate region, while the proposed weighted max-min fair scheduling can effectively ensure the fair access requirements.**

***Index Terms*— Wireless energy transfer (WET), energy beamforming, achievable rate region, finite energy storage and data buffer.**

I. Introduction

RADIO frequency (RF) energy harvesting technology provides a promising routine to realize energy sustainability, which is critical for a massive deployment of energy-constrained wireless systems such as Internet of Things (IoTs) and wireless sensor networks (WSNs). Different from natural resource-based energy harvesting technologies, wireless energy transfer can provide permanent and reliable energy sources for the energy-constrained wireless system without being affected by environmental changes. Although the RF energy transfer technology suffers from low energy efficiency caused by the large-scale fading of RF signals, narrow beams can be used to improve the energy transfer efficiency by employing multiple antennas at the transmitter side, which fits 5G applications of Massive MIMO and millimeter-wave very well [1]. Moreover, 5G technologies based on short-range communications such as ultra-dense networks (UDNs) and device-to-device (D2D) communications can significantly improve the wireless energy transfer efficiency by reducing communication distances. The spectrum is heavily reused in UDNs and D2D communications, resulting in strong co-channel interference, but this co-channel interference can be regarded as a potential energy source for energy-constrained devices [1], which has a huge potential for achieving green 5G networks. Recently, the simultaneous wireless information and power transfer (SWIPT) has evolved as a technical framework to flexibly fulfill the wireless energy transfer (WET) and wireless information transmission (WIT) requirements [2]–[7]. As an example, wireless powered communication network (WPCN) was extensively investigated to effectively support wireless energy-constrained communication [8]–[19]. Basically, the WPCN operates in two phases of downlink WET and uplink WIT. In the downlink WET phase, some energy-constrained nodes harvest energy from the RF signals of some access point (AP). In the successive uplink WIT phase, the nodes use the harvested energy to send their data to the AP. A single antenna WPCN was studied in [8], while the multiple-antenna empowered WPCN was addressed in [10]. In [9] and [11], the full duplex technique was applied in WPCN. User cooperation in the WPCN was studied in [12]–[14], where the user closer to the AP acts as a relay to help the user far away from the AP to forward data in the uplink WIT phase. At the same time, exploiting buffers in the physical layer and link layer has attracted much attention as an effective way to provide new degree of freedom to better schedule the transmission for an improved performance [21]–[23], [25]–[29]. In buffer-aided communication networks, data traffic from higher layer applications can be firstly stored in a data buffer and adaptively transmitted when

Manuscript received December 11, 2018; revised April 27, 2019 and July 12, 2019; accepted August 26, 2019. Date of publication September 10, 2019; date of current version December 10, 2019. The work of X. Lan and Q. Chen was supported in part by the National Natural Science Foundation of China under Grant 61771406 and in part by the Chinese Scholarship Council (CSC). The work of L. Cai was supported in part by the Natural Sciences and Engineering Research Council of Canada (NSERC). The work of L. Fan was supported by the National Natural Science Foundation of China under Grant 61871139. The associate editor coordinating the review of this article and approving it for publication was W. Chen. *(Corresponding author: Qingchun Chen.)*

X. Lan is with the School of Information Science and Technology, Southwest Jiaotong University, Chengdu 611756, China, and also with the Department of Electronics and Communication Engineering, Guangzhou University, Guangzhou 510006, China (e-mail: xiaolonglan1112@gmail.com).

Q. Chen is with the Department of Electronics and Communication Engineering, Guangzhou University, Guangzhou 510006, China (e-mail: qcchen@gzhu.edu.cn).

L. Cai is with the Department of Electrical and Computer Engineering, University of Victoria, Victoria, BC V8W 3P6, Canada (e-mail: cai@ece.uvic.edu).

L. Fan is with the School of Computer Science and Cyber Engineering, Guangzhou University, Guangzhou 510006, China (e-mail: lsfan@gzhu.edu.cn).

Color versions of one or more of the figures in this article are available online at http://ieeexplore.ieee.org.

Digital Object Identifier 10.1109/TWC.2019.2938958

the channels are in good conditions, which leads to either lower energy consumption [16], [17], [20] or larger network throughput [21]–[24] at the cost of some increase in transmission delay. More interestingly, it has been shown in [31] that, unlike the time switching scheme,when the relay is equipped with a data buffer and an energy storage, the optimal time allocation scheme is to allocate an entire time slot for either data transmission or energy harvesting.

Motivated by the great potentials of buffers that are not yet fully explored in WPCN, in this paper, we focus on the buffer-aided WPCN. Unlike the work in [8]–[19], we consider a more realistic scenario, where all terminals are provisioned with a finite energy storage and a finite data buffer. In addition, different data traffic arrival process at different terminals are also considered. Since both the energy storage and the data buffer are finite, there might be data loss due to either the data buffer overflow or the energy storage depletion. For such a system, we focus on how to maximize the long-term average weighted sum rate for all the participating terminals in the WPCN. Basically, different terminals may have quite different data arrival rates in practical application, for instance, different types of sensor devices are deployed to monitor different properties of the surveillance area in WSNs. In order to effectively accommodate heterogenous data rates, the weighted sum rate is considered in the uplink WIT phase of the WPCN. On the basis of the aforementioned problem formulation, the adaptive WPCN design is presented in terms of energy beamforming vector design, power allocations, rate control, time allocations, and the transmission mode selection subject to the average transmit power, peak transmit power, the data loss ratio requirements, as well as the practical data buffer and energy storage constraints. To address this issue, we use the Lyapunov framework to transform the time-average optimization problem into the queue stability problem, which is decomposed into multiple sub-problems to obtain the adaptive design scheme. Our analysis has shown that the proposed adaptive design is asymptotically optimal. And our analysis in this paper unveils that, the proposed adaptive design can substantially improve the average achievable rate region. In addition to heterogeneous data rate requirements, fairness may be another type of access requirement in the practical system. For instance in WSNs, the same type IoT devices are deployed, and their data rates are essentially the same. Now the access point is supposed to collect their data regularly to make system aware of the whole system status. In order to effectively fulfill the fair access requirements, the weighted max-min scheduling design is proposed to ensure that the access rates by all terminals are weighted max-min fair. And the contributions of this paper are two-fold.

- Firstly, the long-term average weighted sum-rate maximization analysis is presented to unveil that, the long-term average achievable rate region of the buffer-aided WPCN system can be substantially improved by carefully considering the energy beamforming vector design, power allocations, rate control, time allocations, and the transmission mode selection, if a certain queuing delay is tolerable.
- Secondly, the weighted max-min long-term achievable rate analysis for all participating terminals unveils that, fair access requirements by different terminals in the buffer-aided WPCN system can be guaranteed. Although there is some loss in the achieved sum rate when compared with the weighted sum-rate maximization design, because now the system has to balance the transmission requirements by different terminals, the long-term average achievable sum-rate can be noticeably improved likewise by considering the energy beamforming vector design, power allocations, rate control, time allocations, and the transmission mode selection.

The remainder of this paper is organized as follows. In Section II, a literature survey is presented to introduce the motivation of our work. The system model of the buffer-aided WPCN is presented in Section III. The long-term average weighted sum-rate maximization design and the weighted max-min fairness scheduling scheme are presented in Section IV and Section V, respectively. Numerical analysis and simulation results are presented in Section VI to verify the effectiveness of our work. Finally, we conclude this paper in Section VII.

Notations: All boldface letters indicate vectors (lower case) or matrices (upper case). The superscripts $(\cdot)^T$, $(\cdot)^H$ denote the transpose and the conjugate transpose. $|z|$ denotes the magnitude of a complex variable z, $||\mathbf{z}||$ denote the Euclidean norm of a complex vector $\mathbf{z}$, $\mathrm{tr}(\mathbf{A})$ denotes the trace of a matrix $\mathbf{A}$, where $\mathbf{A} \succeq 0$ indicates that matrix $\mathbf{A}$ is positive semidefinite. $\mathbf{A} = \mathrm{diag}(\mathbf{v})$ denotes a square diagonal matrix with the elements of vector $\mathbf{v}$ on the main diagonal. $y = O(x)$ denotes y going to 0 as x approaches 0.

II. Related Works

SWIPT provides a promising and energy sustainable framework to realize information transmission. Two practical receiver architectures were proposed in [2] to realize SWIPT via either time switching (TS) or power splitting (PS). SWIPT over wireless channels has been extensively studied [2]–[7]. Based on the TS and PS receiver architectures, two relay protocols for RF energy harvesting networks were proposed in [3]. The performance of three nodes in a multiple-input multiple-out wireless broadcast system was studied in [4], where one receiver harvests energy and another receiver decodes information separately from the signals sent by a common transmitter. A multiuser multiple-input single-output interference channel was considered in [6] and [7], where the received signal is subdivided for energy harvesting (EH) and data transmission, the transmit beamforming vectors and receive PS ratio were jointly designed to minimize the total transmission power subject to both signal-to-interference-plus-noise ratio and EH constraints.

Wireless powered communication networks with single AP and multiple users for joint downlink WET and uplink WIT have been extensively studied in [8]–[19]. A "*harvest-then-transmit*" protocol was proposed in [8], in which all terminals first harvest the wireless energy from the single antenna AP

in the downlink WET phase and then transmit their data to the AP in the uplink WIT phase by using the harvested RF energy in a TDMA manner. It is shown that the time allocated to the downlink WET and the uplink WIT can be jointly optimized to maximize the sum throughput. Moreover, an interesting "*doubly near-far*" phenomenon was revealed in [8], that is, when a user far away from the AP receives less wireless energy than a user closer to the AP in the downlink WET phase, it has to transmit with more power in the uplink WIT phase to overcome the larger path loss. Furthermore, in order to ensure all users are allocated with an equal rate in their uplink information transmissions, a new algorithm was proposed in [8] to overcome the doubly near-far problem. The work in [8] was later extended to WPCN with a multi-antenna AP in [10], where the time allocation, downlink energy beamforming, uplink transmit power allocations, as well as receiver beamforming, are jointly optimized to maximize the minimum throughput among all users. Full duplex (FD) technique was applied to the WPCNs in [9], where the AP is equipped with two antennas, one is used for broadcasting energy and the other one for receiving data from users at the same time. The time allocations to the AP for downlink WET and users for uplink WIT, as well as the transmit power allocations at the AP are jointly optimized to maximize the weighted sum rate of the full duplex system.

User cooperation between two users was considered in [12]–[14], where the user who is close to the AP and thus with better downlink and uplink channels uses part of its allocated uplink time and downlink harvested energy to help the distant user forward data to the AP. In [12], the time and power allocations were considered to maximize the weighted sum rate of two users. By further extending the work in [12], the AP equipped with multiple antennas was considered in [13] and [14], where the energy beamforming, time and power allocation were jointly optimized to maximize the weighted sum-rate. The users equipped with infinite and finite energy storage was considered for the WPCN in [15], where the time and power allocations were jointly optimized to maximize the sum rates. It is revealed that, when a user is equipped with energy storage, the power allocation can be realized adaptively based on channel condition and the harvested energy in the previous time slots, which can substantially improve the sum rate performance. Every terminal equipped with energy storage and data buffer was considered in [16] for the WPCN, where the energy beamforming vector, the data scheduling and the data transmit power were jointly designed to minimize the expected transmit power for the given data generation rate. The power-delay tradeoff for the WPCN was investigated in [17]. For the buffer-aided communication networks, an adaptive link selection scheme was proposed in [22] for the buffer-aided relay network to improve performance, this is because the link with better channel state information (CSI) will always be selected. A three node wireless powered relay network was studied in [27], where the relay is provisioned with both data buffer and energy storage. It is shown that the buffer-aided relay can effectively improve the achievable transmission throughput. Two-way wireless power buffer-aided relay network was considered in [24] to maximize the

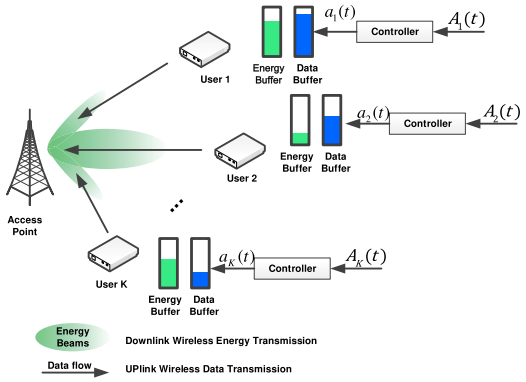

Fig. 1. Wireless powered communication network with downlink energy beamforming and uplink data transmission.

long-term average rate region. The throughput maximization problem of energy harvesting two-way communication network with finite batteries and finite data buffers was considered in [28]. A multi-hop sensor network with finite energy storage and data buffer was studied in [29], where the data queue and battery storage were jointly controlled to maximize the long-term average sensing rate under certain QoS constraints.

As a representative use case in the emerging IoT and WSN system, how to jointly balance the WET and WIT design to fulfill specific application requirement and how to adapt to different environment impose critical challenges on the WPCN technique. Previous research efforts have demonstrated how to devise the WPCN with different settings, for instance, the WPCN with either single antenna AP or multiple antenna AP, the half-duplex WPCN and the full-duplex WPCN. Meanwhile, the energy beamforming, the time allocation and the transmit power allocation are included in the WPCN design for a desired performance. Nonetheless, one may also notice that, there are not so many research results regarding the buffer-aided WPCN. The recent progress in the buffer-aided wireless communication has explicitly confirmed us the great potential of the "*receive-schedule-transmit*" transmission policy enabled by the utilized data buffer. In this paper, we focus on the buffer-aided WPCN, where all terminals are provisioned with a finite energy storage and a finite data buffer. Besides, different data traffic arrival process at different terminals are also considered to characterize realistic data arrival rates. Furthermore, fair access requirements by different terminals in the practical system are also considered. In the following Section III, we will explicitly formulate the problem we consider in this paper.

III. System Model

A. Network Model

We consider a wireless powered communication network with WET in the downlink and WIT in the uplink, as depicted in Fig. 1. The network consists of one AP and K terminals denoted by $U_k, k \in [1, K]$. We assume that the AP is equipped with N antennas, each terminal has a single antenna, both the AP and K terminals operate in the same frequency band. In addition, each terminal is an energy constrained node that

is powered by the WET from the AP only. Recent research work in [33] has shown that, when compared with the TDMA-based WPCN, the non-orthogonal multiple access (NOMA) based WPCN scheme not only consumes more energy, but also tends to be less spectral efficiency. Therefore, we consider the TDMA-based WPCN in this paper. Namely, all K terminals are supposed to transmit their independent data to the AP regularly in a TDMA manner by using their harvested RF energy. We assume that U_k is provisioned with one finite energy storage (rechargeable battery) B_{ek} with limited capacity $\hat{E}_k$ and one finite data buffer B_{dk} with limited size $\hat{Q}_k$. As shown in Fig. 1, we introduce a controller at every user to specify the data arrival rate at which data are placed in the data buffer B_{dk}. We consider a time slotted system and in the t-th time slot, the amount of data from the upper application for U_k is denoted by $A_k(t)$, which is upper bounded by $\hat{A}_k$, $(0 < \hat{A}_k < \infty)$. Let $a_k(t)$ denote the amount of data for U_k that are actually placed in B_{dk} at slot t. The queue state of B_{ek} and B_{dk} at slot t is denoted by $E_k(t)$ and $Q_k(t)$, respectively. All links are assumed to be block fading such that the channel coefficients are constant within each time slot but may change independently from one to another. Meanwhile, we assume that all channels are reciprocal and the AP can obtain the perfect channel state information (CSI). Let $\mathbf{g_k(t)} \in \mathbb{C}^{1\times N}$ denote the channel coefficient vector from the AP to U_k in the t-th time slot, and we let $\hat{g}_k = \max_t\{||\mathbf{g_k(t)}||^2\}$.

For the considered WPCN, two transmission modes are assumed: (i). RF energy transmission mode in which the AP transmits RF energy beams to K terminals; (ii). data transmission mode in which K terminals transmit their independent data to the AP in a TDMA manner. A binary variable of $d(t) \in \{0, 1\}$ is introduced to indicate whether or not the corresponding transmission mode is selected at time t. $d(t) = 0$ if the RF energy transmission mode is selected; otherwise the data transmission mode is selected. In this paper, the centralized scheduling scheme is assumed, in which the AP can be used to obtain the data and energy queue state information of all terminals, and the CSIs of all links. In fact, all the terminals know their data and energy queue state information. By designing a suitable signaling system, it is assumed that all the terminals can feed back their data and energy queue state information back to the AP. The CSI acquisition requires proper insertion of channel estimation pilots at the terminals and the appropriate channel estimation design at the AP. Since the focus of this paper is to design the adaptive transmission scheduling scheme based on the current data and energy state information and CSI, we assume that the AP can obtain perfect CSI. For the realistic WPCN with either imperfect or outdated CSI, we need to design a robust adaptive transmission scheme to approach the performance with the ideal CSI, which will be explored in the future. At the beginning of each time slot, we assume that the AP can make up decision based on the collected data and energy queue state information and CSI, and inform all the relevant terminals how to adjust their energy harvesting or transmission. The symbol notations used throughout the paper are summarized in TABLE I.

TABLE I
SYMBOL NOTATION LIST

Symbol	Definition
$Z(t)$	Average transmit power consumption queue of the AP
$Q_k(t), \tilde{Q}_k(t)$	The actual and virtual data queue length of U_k at time t
$E_k(t), \tilde{E}_k(t)$	The actual and virtual energy queue length of U_k at time t
$\hat{Q}_k, \hat{E}_k$	The maximum data buffer size and energy storage size of U_k
$A_k(t)$	At time t, the amount of data from the upper application for the U_k
$a_k(t)$	The amount of data for U_k that are actually placed in the corresponding data buffer at time t
$\mathbf{g_k(t)}$	Channel coefficient vector from the AP to U_k at time t
$\mathbf{w(t)}$	Energy beamforming vector at time t
ζ	Energy conversion efficiency
$H_k(t)$	Harvested energy by U_k at time t
$P_k(t)$	Transmit power of U_k at time t
P_c	Circuit power consumption at terminals
$R_k(t)$	Data transmission rate from U_k to AP at time t
$C_k(t)$	Energy consumption of U_k at time t
$P_{\max}, \bar{P}_{\max}$	Peak transmit power and the maximal allowed time average transmit power budget at the AP
P_{loss}^k	Long-term data loss ratio of U_k
$D_k(t)$	The amount of data loss of U_k at time t
P_0^k	The frequency of the energy state is below E_k^{re} for U_k
$I_0^k(t)$	An indicator that the energy state of U_k is less than E_k^{re} at time t
η_d^k	The maximal allowed long-term data loss ratio for U_k
η_0^k	The maximal allowed frequency of energy state that is below the desired energy E_k^{re} for U_k
$L_k(t)$	The amount of dummy data transmitted if there is no enough data to be sent
$M_k(t)$	The amount of missed replenishing energy due to the full energy storage at time t
Ω_k	Average arrival rate of U_k

B. RF Energy Transmission Mode

Within time slot t, if we have the following energy beamforming vector and transmit power at the AP

$$\mathbf{w(t)} = (w_1(t), w_2(t), \ldots, w_N(t))^T \in \mathbb{C}^{N\times 1},$$
$$P(t) = ||\mathbf{w(t)}||^2 = \mathbf{w^H(t)w(t)} = \mathbf{tr(w(t)w^H(t))}, \quad (1)$$

the received signal at K terminals can be given by [10]

$$\mathbf{y(t)} = \mathbf{G(t)w(t)} + \mathbf{n(t)}, \quad (2)$$

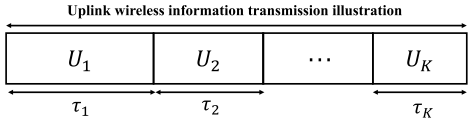

Fig. 2. Time allocation in the uplink WIT phase.

where $\mathbf{G(t)} = [\mathbf{g_1^T(t)}, \ldots, \mathbf{g_K^T(t)}]^T$, $\mathbf{y(t)} = [y_1(t), \ldots, y_K(t)]^T$ and $\mathbf{n(t)} = [n_1(t), \ldots, n_K(t)]^T$. $y_k(t)$ and $n_k(t)$ denotes the received signal and noise at U_k, respectively. $n_k(t) \sim \mathcal{CN}(0, \sigma^2)$. Basically, the harvested energy from the noise can be ignored. The harvested energy by U_k is

$$\begin{aligned} H_k(t) &= (1 - d(t))\zeta\mathcal{T}|\mathbf{g_k(t)w(t)}|^2 \\ &= (1 - d(t))\zeta\mathcal{T}\mathbf{tr}(\mathbf{g_k^H(t)g_k(t)w(t)w^H(t)}), \end{aligned} \quad (3)$$

where ζ denotes the energy conversion efficiency, $\mathcal{T}$ is the time slot duration. For simplicity, we assume a normalized unit time slot, namely, $\mathcal{T} = 1$.

C. Data Transmission Mode

In the uplink data transmission mode, the duration $\mathcal{T}$ of one time slot will be further subdivided into K sub-slots, during which K terminals transmit their independent data to the AP in a TDMA manner, as shown in Fig. 2. The amount of time assigned to terminal U_k in time slot t is denoted by $\tau_k(t)$, $0 \le \tau_k(t) \le 1$, $k = 1, 2, \ldots K$. And we have

$$\sum_{k=1}^{K} \tau_k(t) = 1. \quad (4)$$

For the k-th data transmission sub-slot, U_k transmits the data from B_{dk} to the AP by using the harvested energy in B_{ek}. Let $x_k(t)$ denote the transmit signal by U_k satisfying $\mathbb{E}[|x_k(t)|^2] = 1$. Thus the received signals at AP is

$$\mathbf{y_{A,k}(t)} = \sqrt{P_k(t)}\mathbf{g_k^T(t)}x_k(t) + \mathbf{n_{A,k}(t)}, \quad k = 1, 2, \cdots, K, \quad (5)$$

where $P_k(t)$ represents the transmit power by U_k, $\mathbf{y_{A,k}(t)} \in \mathbb{C}^{N\times 1}$ and $\mathbf{n_{A,k}(t)} \in \mathbb{C}^{N\times 1}$ stands for the received signal and noise at the AP, respectively. It is assumed that $\mathbf{n_{A,k}(t)} \sim \mathcal{CN}(\mathbf{0}, \sigma^2\mathbf{I}_N), \forall k$, where $\mathbf{I}_N$ is an $N \times N$ identity matrix. Let $R_k(t)$ denote the data transmission amount from U_k to AP at time t, and we have

$$R_k(t) = d(t)\tau_k(t)\log_2\left(1 + \frac{P_k(t)||\mathbf{g_k(t)}||^2}{\sigma^2}\right), \quad k = 1, 2, \cdots, K. \quad (6)$$

D. Energy Queue and Data Queue Update Model

Each terminal has a finite size energy storage for storing the harvested RF energy. When scheduled for RF energy transmission at slot t, each terminal harvests the RF energy from the AP and stores it in its energy storage. When scheduled for data transmission at slot t, each terminal sends data to the AP by using energy stored in its energy storage. Let P_c denote a constant circuit power consumption at the user terminal for operating its transmit filter, frequency synthesizer, and so on [32], [33]. Without loss of generality, we assume that all users have the same circuit power consumption. Therefore, the energy queue evolution and the data queue evolution of U_k can be given by

$$E_k(t+1) = \min\left[E_k(t) + H_k(t) - C_k(t), \hat{E}_k\right], \quad (7a)$$

$$Q_k(t+1) = \min\left[(Q_k(t) - R_k(t))^+ + a_k(t), \hat{Q}_k\right], \quad (7b)$$

where $(\cdot)^+ = \max[\cdot, 0]$, $C_k(t) = d(t)\tau_k(t)(P_k(t) + P_c)$ denotes the energy consumption of U_k in time slot t.

IV. Long-Term Average Weighted Sum-Rate Maximization Design

In this section, our objective is to maximize the long-term average weighted sum-rate (WSR) subject to the long-term and peak transmit power constraint, and the practical constraints on both the data buffer and energy storage. When the terminal is equipped with data buffer and energy storage, a transmission mode can be adaptively selected based on the current CSIs as well as the data and energy queue state information. Moreover, energy beamforming design, the optimal power allocations, rate control, time allocations, and the transmission mode selection are jointly considered for the sake of maximizing the long-term average weighted sum-rate. And the long-term average weighted sum-rate maximization problem can be formulated as below

$$\begin{aligned}
(\mathcal{P}\mathbf{1}): &\max_{\mathbf{w(t)}, P_k(t), a_k(t), \tau_k(t), d(t)} \liminf_{T\to\infty} \frac{1}{T}\sum_{t=0}^{T-1}\sum_{k=1}^{K}\theta_k a_k(t) \\
\text{s.t. } & C1: Q_k(t+1) = \min\left[\left(Q_k(t) - R_k(t)\right)^+ + a_k(t), \hat{Q}_k\right], \\
& \qquad \forall k, t, \\
& C2: E_k(t+1) = \min\left[E_k(t) + H_k(t) - C_k(t), \hat{E}_k\right], \quad \forall k, t, \\
& C3: 0 \le a_k(t) \le A_k(t), \quad \forall k, t, \\
& C4: 0 \le C_k(t) \le E_k(t), \quad \forall k, t, \\
& C5: 0 \le ||\mathbf{w(t)}||^2 \le P_{\max}, \quad \forall t, \\
& C6: \limsup_{T\to\infty} \frac{1}{T}\sum_{t=0}^{T-1}(1 - d(t))||\mathbf{w(t)}||^2 \le \bar{P}_{\max}, \\
& C7: P_{loss}^k \le \eta_d^k, \quad \forall k, \\
& C8: P_0^k \le \eta_0^k, \quad \forall k, \\
& C9: 0 \le \tau_k(t) \le 1, \quad \forall k, t, \\
& C10: \sum_{k=1}^{K}\tau_k(t) = 1, \quad \forall t, \\
& C11: d(t)(1 - d(t)) = 0, \quad \forall t,
\end{aligned}$$

where the weighting coefficient θ_k is utilized to fulfill different data rate requirements by different terminals. The long-term achievable rate region can be determined by maximizing the above long-term average weighted sum rate for all possible weighting coefficients $\theta_k \in [0, 1]$ and $\sum_{k=1}^{K}\theta_k = 1$ [9], [30]. In particular, the maximum long-term average sum rate can be achieved when $\theta_1 = \theta_2 = \cdots = \theta_K = \frac{1}{K}$ [30]. $P_{\max}$ and $\bar{P}_{\max}$ denotes the peak transmit power and the maximally allowed average transmit power budget at the AP,

respectively. P_{loss}^k is the long-term data loss ratio of U_k [29], and

$$P_{loss}^k = \begin{cases} 0, \\ \quad \text{if} \quad \liminf_{T\to\infty} \frac{1}{T} \sum_{t=0}^{T-1} a_k(t) = 0, \\ \limsup_{T\to\infty} \frac{\sum_{t=0}^{T-1} D_k(t)}{\sum_{t=0}^{T-1} a_k(t)}, \\ \quad \text{otherwise}, \end{cases} \tag{8}$$

where $D_k(t) = \left(\left(Q_k(t) - R_k(t)\right)^+ + a_k(t) - \hat{Q}_k\right)^+$ is the amount of data loss in the t-th time slot at U_k. η_d^k is the maximally allowed data loss ratio by U_k. P_0^k is the frequency that the energy state is below the certain desired value for U_k, and

$$P_0^k = \limsup_{T\to\infty} \frac{1}{T} \sum_{t=0}^{T-1} I_0^k(t), \tag{9}$$

where $I_0^k(t)$ is the indicator that the energy state of U_k is less than the desired energy E_k^{re}, and

$$I_0^k(t) = \begin{cases} 0, & \text{if } E_k(t) - C_k(t) > E_k^{re}, \\ 1, & \text{otherwise.} \end{cases} \tag{10}$$

η_0^k is the maximally allowed frequency that the energy state is below E_k^{re}. $C1$ and $C2$ stands for the data queue and energy queue evolution constraint, respectively. $C3$ indicates that the amount of data that are actually placed in the data buffer cannot exceed the amount of data from the upper application. $C4$ ensures that the energy consumed in each time slot does not exceed the energy stored in the energy storage. $C5$ and $C6$ stands for the peak transmit power constraint and the average transmit power constraint, respectively. $C7$ specifies that the long-term data loss ratio of U_k cannot exceed η_d^k. $C8$ corresponds to the frequency that the energy state is below the desired value should not exceed η_0^k. $C9$ and $C10$ stand for the time allocation constraints in the data transmission mode. $C11$ specifies the transmission mode selection constraint.

A. Virtual Queue Analysis

To incorporate our analysis in the Lyapunov optimization framework, we define $\tilde{Q}_k(t)$, $\tilde{E}_k(t)$, and $Z(t)$ as the virtual data queue, the virtual energy queue, and the average transmit power consumption queue of the AP, respectively, and their queue evolutions can be given by

$$\tilde{Q}_k(t+1) = \left(\tilde{Q}_k(t) + (1-\eta_d^k)a_k(t) - R_k(t) + L_k(t)\right)^+, \quad \forall k, \tag{11}$$

$$\tilde{E}_k(t+1) = \min\left(\tilde{E}_k(t) + \xi\eta_0^k + H_k(t) - C_k(t) - M_k(t) - \xi I_0^k(t), \phi_k\right), \quad \forall k, \tag{12}$$

$$Z(t+1) = \left(Z(t) + (1-d(t))||\mathbf{w}(\mathbf{t})||^2 - \bar{P}_{\max}\right)^+, \tag{13}$$

where $L_k(t) = \left(R_k(t) - Q_k(t)\right)^+$ represents the amount of dummy data sent by using the allocated energy when the data is insufficient in B_{dk}, $M_k(t) = \left(E_k(t) + H_k(t) - C_k(t) - \hat{E}_k(t)\right)^+$ represents the amount of supplemental energy missed due to the energy buffer being full. $\xi > 0$ is a scaled coefficient selected to ensure that $\xi\eta_0^k$ and the harvested energy are in the same order of magnitude. ϕ_k is the maximal virtual energy queue size, i.e., $\phi_k \geq \tilde{E}_k(t)$. So we have $\phi_k - \tilde{E}_k(t+1) = (\phi_k - \tilde{E}_k(t) - \xi\eta_0^k - H_k(t) + C_k(t) + M_k(t) + \xi I_0^k(t))^+$. It is worth noting that the length of virtual energy queue $\tilde{E}_k(t)$ can be less than 0. Fig. 3(a) illustrates the relationship between the actual and virtual data queues. The virtual data queue can be sub-divided into two parts, the first part depicts the actual data queue evolution, the other characterizes the QoS requirement on the data queue. Fig. 3(b) shows the relationship between the virtual queue $\phi_k - \tilde{E}_k(t)$ and the actual energy queue. The virtual queue $\phi_k - \tilde{E}_k(t)$ consists of two parts as well, the first part characterizes the actual energy queue evolution process and the other one specifies the QoS requirement on the energy queue. On the other hand, the length of the virtual queue $\tilde{Q}_k(t)$ and $\tilde{E}_k(t)$ also increases (decreases) as the length of actual queue $Q_k(t)$ and $E_k(t)$ increases (decreases). $\phi_k - \tilde{E}_k(t)$ increases (decreases) as actual energy queue $E_k(t)$ decreases (increases) or the frequency that energy state is below the desired value increases (decreases). $Z(t)$ increases as the energy consumption of the AP increases. The virtual queues $\tilde{Q}_k(t)$, $\phi_k - \tilde{E}_k(t)$, and $Z(t)$ satisfy Lindley's queue evolutions, thus it is reasonable to expect the stability of the virtual queues, which implies that QoS constraints on data and energy buffers, together with the average energy consumption of the AP, can be satisfied.

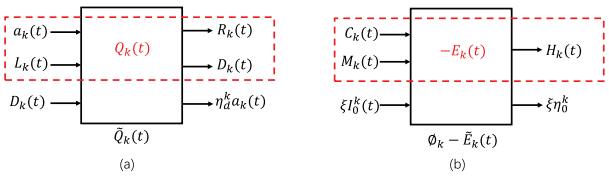

Fig. 3. Actual and virtual data buffer and energy storage queues.

Lemma 1: If the virtual queues $\tilde{Q}_k(t)$, $\tilde{E}_k(t)$, and $Z(t)$ are all rate stable, *i.e.*,

$$\lim_{T\to\infty} \frac{\tilde{Q}_k(T)}{T} = \lim_{T\to\infty} \frac{\tilde{E}_k(T)}{T} = \lim_{T\to\infty} \frac{Z(T)}{T} = 0,$$

then $P_{loss}^k \leq \eta_d^k$, $P_0^k \leq \eta_0^k$ and $\limsup_{T\to\infty} \frac{1}{T} \sum_{t=0}^{T-1} (1 - d(t))||\mathbf{w}(\mathbf{t})||^2 \leq \bar{P}_{\max}$ can be satisfied.

Proof: Due to the space limit, the detailed proof can be found in Appendix A in https://www.researchgate.net/publication/329527135_Buffer-aided_Adaptive_Wireless_Powered_Communication_Network_with_Finite_Energy_Storage_and_Data_Buffer [34]. ■

Lemma 1: indicates that we can transform the QoS constraints on data buffer and energy storage, as well as the time average power consumption constraint, into a queue stability problem. Therefore, to ensure that all virtual queues are stable, we can use the Lyapunov optimization framework to solve $\mathcal{P}\mathbf{1}$.

B. Lyapunov Optimization Framework

Based on the virtual data buffer state, virtual energy storage state, and virtual average power consumption, we define the

following quadratic Lyapunov function

$$L(\mathbf{\Theta(t)})=\frac{1}{2}\sum_{k=1}^{K}\left[\mu_{1k}\tilde{Q}_k^2(t)+\mu_{2k}(\phi_k-\tilde{E}_k(t))^2\right]+\frac{\mu_3}{2}Z^2(t), \tag{14}$$

where $\mathbf{\Theta(t)}=[\{\tilde{E}_k(t)\}|_{k=1}^K,\{\tilde{Q}_k(t)\}|_{k=1}^K,Z(t)]$ denotes the concatenated vector of all virtual queues, μ_{1k}, $\mu_{2k}, k=1,2,\cdots,K$ and μ_3 are nonnegative constants. The value $L(\mathbf{\Theta(t)})$ is a scalar measure of the current virtual queue length, which is defined to grow larger as the queue system moves towards undesirable states. $L(\mathbf{\Theta(t)})$ grows larger as $\tilde{Q}_k(t)$ and $Z(t)$ increases, or $\tilde{E}_k(t)$ decreases. We may use the following Lyapunov drift to represent the change in the Lyapunov function between two consecutive time slots

$$\Delta(\mathbf{\Theta(t)})=L(\mathbf{\Theta(t+1)})-L(\mathbf{\Theta(t)}). \tag{15}$$

To ensure that all the virtual queues are stable, it is desirable to minimize the above Lyapunov drift for the given $\mathbf{\Theta(t)}$. On the other hand, our objective is to maximize the long-term average weighted sum-rate, so we can follow the Lyapunov optimization framework to minimize the following Lyapunov drift-plus-penalty

$$\Delta(\mathbf{\Theta(t)})-V\sum_{k=1}^{K}\theta_k a_k(t), \tag{16}$$

where V is a nonnegative control parameter, which can be utilized to realize a tradeoff between the average virtual queue size and the average weighted sum-rate. We may notice that the Lyapunov drift-plus-penalty is a multi-objective function, the first part is the Lyapunov drift to ensure the stability of all the queues, and the second part is the weighted sum rate. Thus, we minimize the Lyapunov drift-plus-penalty to ensure that the queue stability and the maximum weighted sum rate can be achieved at the same time.

Lemma 2: The Lyapunov drift-plus-penalty function can be upper bounded by

$$\begin{aligned}
&\Delta(\mathbf{\Theta(t)})-V\sum_{k=1}^{K}\theta_k a_k(t)\\
&\le B+\sum_{k=1}^{K}\Big\{\mu_{1k}\tilde{Q}_k(t)\big((1-\eta_d^k)a_k(t)-R_k(t)+L_k(t)\big)\\
&\quad+\mu_{2k}(\phi_k-\tilde{E}_k(t))\big(-\xi\eta_0^k-H_k(t)+C_k(t)\\
&\quad+M_k(t)+\xi I_o^k(t)\big)\Big\}\\
&\quad+\mu_3 Z(t)\big((1-d(t))||\mathbf{w(t)}||^2-\bar{P}_{\max}\big)-V\sum_{k=1}^{K}\theta_k a_k(t),
\end{aligned} \tag{17}$$

where $B=\frac{1}{2}\big\{\sum_{k=1}^{K}\big(\mu_{1k}\big((1-\eta_d^k)\hat{A}_k\big)^2+\mu_{1k}(\hat{R}_k)^2+\mu_{2k}(\xi\eta_0^k+\hat{H}_k)^2+\mu_{2k}(\xi+\hat{C}_k)^2\big)+\mu_3(P^{max})^2+\mu_3(\bar{P}^{\max})^2\big\}$, $\hat{A}_k$, $\hat{R}_k$, $\hat{H}_k$ and $\hat{C}_k$ denotes the maximal arrival rate of U_k from the applications, the maximal transmission rate from the U_k to AP, the maximal harvested energy, and the maximal energy consumption of the U_k, respectively.

Proof: Due to the space limit, the detailed proof can be found in Appendix B in https://www.researchgate.net/publication/329527135_Buffer-aided_Adaptive_Wireless_Powered_Communication_Network_with_Finite_Energy_Storage_and_Data_Buffer [34]. ■

To ensure that both the maximal average weighted sum-rate and the virtual queue stability can be realized simultaneously, we should minimize the Lyapunov drift-plus-penalty in (16). ***Lemma 2*** provides us an upper bound on the Lyapunov drift-plus-penalty, and we solve the following optimization problem instead of directly minimizing the Lyapunov drift-plus-penalty item. At each time slot t, given the current virtual queue state $\mathbf{\Theta(t)}$ and the current channel state information, we make decisions on rate control, energy beamforming, time allocations, power allocations, and mode selection by solving the following optimization problem:

$$\begin{aligned}
(\mathcal{P}\mathbf{2}):\ \min_{\mathbf{w},P_k,a_k,\tau_k,d}\ &\sum_{k=1}^{K}\Big\{\mu_{1k}\tilde{Q}_k(t)\big((1-\eta_d^k)a_k(t)-R_k(t)\big)\\
&+\mu_{2k}(\phi_k-\tilde{E}_k(t))\big(-H_k(t)+C_k(t)\big)\Big\}\\
&+\mu_3 Z(t)(1-d(t))||\mathbf{w}(t)||^2-V\sum_{k=1}^{K}\theta_k a_k(t)\\
\text{s.t.}\ \ &C3\sim C5, C9\sim C11.
\end{aligned} \tag{18}$$

It is worth noting that variable $a_k(t)$ is independent of other variables, and thus we can decompose the above optimization problem to obtain the optimal rate control policy. On the other hand, optimization variable $d(t)$ is a binary variable, and only two transmission modes can be chosen. Therefore, we can enumerate the optimization problem in different cases. If $d(t)=0$ we can design the optimal energy beamforming in the RF energy transmission mode, and if $d(t)=1$ we can obtain the optimal power and time allocations in the data transmission mode.

C. Rate Control

In order to obtain the optimal rate control, $\mathcal{P}\mathbf{2}$ can be decomposed as follows

$$\begin{aligned}
&\min_{a_k(t)}\ \sum_{k=1}^{K}\big(\mu_{1k}\tilde{Q}_k(t)(1-\eta_d^k)-\theta_k V\big)a_k(t),\\
&s.t.\ \ 0\le a_k(t)\le A_k(t)\ \ \forall k,t.
\end{aligned} \tag{19}$$

Since the objective function and the constraint function in the above optimization problem are both linear, the optimal solution can be obtained at the boundary only. Thus, the optimal rate control scheme is given in ***Lemma 3***.

Lemma 3: The optimal rate control of U_k is given by

$$a_k(t)=\begin{cases}A_k(t), & \text{if } \theta_k V>\mu_{1k}\tilde{Q}_k(t)(1-\eta_d^k),\\ 0, & \text{otherwise.}\end{cases} \tag{20}$$

Lemma 3 indicates that if a higher data loss ratio η_d^k is allowed, then more data will be placed in the data buffer B_{dk}. In addition, if the virtual data queue $\tilde{Q}_k(t)$ is larger, less data will be placed in the data buffer B_{dk}.

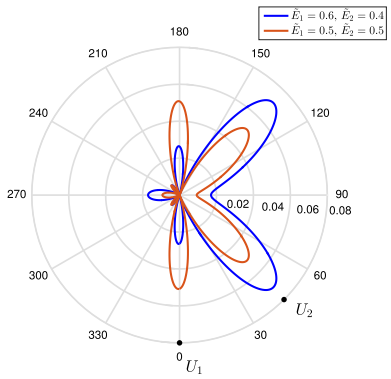

Fig. 4. The antenna radiation patterns of the uniform linear array when $\phi_k = 1$, $\mu_{2k} = 2 \times 10^{11}$, $\mu_3 = 100$, $\zeta = 0.5$ and $Z(t) = 10$.

D. Energy Beamforming Design

If the RF energy transmission mode is selected, namely, $d(t) = 0$, the original optimization problem $\mathcal{P}\mathbf{2}$ can be reformulated as

$$\min_{\mathbf{w(t)}} \; -\sum_{k=1}^{K} \mu_{2k}(\phi_k - \tilde{E}_k(t))|\mathbf{g_k(t)w(t)}|^2\zeta + \mu_3 Z(t)||\mathbf{w(t)}||^2$$
$$s.t. \;\; ||\mathbf{w(t)}||^2 \le P_{\max}. \tag{21}$$

Lemma 4: The optimal energy beamforming is given by

$$\mathbf{w(t)} = \begin{cases} \mathbf{0}, & \text{if } \; f_{\min}(t) \ge 0, \\ \sqrt{P_{\max}}\mathbf{u_1(t)}, & \text{otherwise}, \end{cases} \tag{22}$$

where $f_{\min}(t)$ is the smallest eigenvalue corresponding to matrix $\mathbf{F(t)} = \mu_3 Z(t)\mathbf{I} - \sum_{k=1}^{K} \mu_{2k}(\phi_k - \tilde{E}_k(t))\zeta \mathbf{G_k(t)}$, $\mathbf{G_k(t)} = \mathbf{g_k^H(t)g_k(t)}$ and $\mathbf{u_1(t)}$ is a eigenvalue vector corresponding to the smallest eigenvalue $f_{\min}(t)$. In addition, since the smallest eigenvalue may not be unique, the optimal energy beamforming vector $\mathbf{u_1(t)}$ may not be unique.

Proof: Due to the space limit, the detailed proof can be found in Appendix C in https://www.researchgate.net/publication/329527135_Buffer-aided_Adaptive_Wireless_Powered_Communication_Network_with_Finite_Energy_Storage_and_Data_Buffer [34]. ∎

In Fig. 4, we illustrate the relationship between the virtual energy queue length and the harvested energy. In this figure, we assume that the AP is equipped with four antennas and a uniform linear array is used. The channel coefficient vector $\mathbf{g_k}(t) = \sqrt{d_k^{-m}}\mathbf{g_k^{an}}$ with $\mathbf{g_k^{an}} = [1 \; e^{j\vartheta_k} \; e^{j2\vartheta_k} \; \cdots \; e^{j(N-1)\vartheta_k}]$, where d_k denotes the distance between the AP and U_k, m is the path loss exponent and $\vartheta_k = -\frac{2\pi d^{an}\sin(\varphi_k)}{\lambda}$, d^{an} is the spacing between successive antenna elements at the AP, λ is the wavelength of RF energy signal, and φ_k is the direction of U_k to the AP. There are two users that are 5 m away from the AP. We set $P_{\max} = 30$ dBm, $m = 2$, $d^{an} = \frac{\lambda}{2}$, and $\{\varphi_1, \varphi_2\} = \{0°, 45°\}$. As shown in Fig. 4, we can observe that less energy will be directed to U_1 than to U_2 when $\tilde{E}_2 < \tilde{E}_1$ and even energy can be directed to both U_1 and U_2 when $\tilde{E}_2 = \tilde{E}_1$.

E. Time and Power Allocation in Data Transmission Mode

In the data transmission mode, all users transmit their independent data to the AP in the TDMA manner. We have $d(t) = 1$, the original optimization problem $\mathcal{P}\mathbf{2}$ can be rewritten as

$$\min_{P_k(t),\tau_k(t)} \; \sum_{k=1}^{K} \Big[-\mu_{1k}\tilde{Q}_k(t)\tau_k(t)\log_2\Big(1+\frac{P_k(t)||\mathbf{g_k(t)}||^2}{\sigma^2}\Big) + \mu_{2k}(\phi_k - \tilde{E}_k(t))(P_k(t)+P_c)\tau_k(t)\Big]$$
$$\text{s.t.} \;\; 0 \le \tau_k(t)(P_k(t)+P_c) \le E_k(t),$$
$$\sum_{k=1}^{K}\tau_k(t) = 1, \;\; \tau_k(t) \ge 0. \tag{23}$$

Based on the above optimization problem, the optimal time allocations and power allocations in the data transmission mode are derived in the following Lemma 5.

Lemma 5: The optimal time and power allocation in the data transmission mode are given by

$$\tau_k(t) = \begin{cases} 1, & \text{if } k = \arg\min_{i\in\{1,2,\cdots,K\}} \Lambda_i(t), \\ 0, & \text{otherwise}, \end{cases} \tag{24}$$

and

$$P_k(t) = \begin{cases} \min\Big[\Big(\frac{\mu_{1k}\tilde{Q}_k(t)}{\mu_{2k}\left(\phi_k - \tilde{E}_k(t)\right)\ln 2} - \frac{\sigma^2}{||\mathbf{g_k(t)}||^2}\Big)^+, \\ \quad (E_k(t) - P_c)^+\Big], \text{if } k = \arg\min_{i\in\{1,2,\cdots,K\}} \Lambda_i(t), \\ 0, \quad \text{otherwise}. \end{cases} \tag{25}$$

where

$$\Lambda_k(t) = -\mu_{1k}\tilde{Q}_k(t)\log_2\left(1+\frac{e_k(t)||\mathbf{g_k(t)}||^2}{\sigma^2}\right) + \frac{\mu_{1k}\tilde{Q}_k(t)e_k(t)||\mathbf{g_k(t)}||^2}{\left(e_k(t)||\mathbf{g_k(t)}||^2 + \sigma^2\right)\ln 2}, \tag{26}$$

$$e_k(t) = \min\left[\left(\frac{\mu_{1k}\tilde{Q}_k(t)}{\left(\mu_{2k}(\phi_k - \tilde{E}_k(t))\right)\ln 2} - \frac{\sigma^2}{||\mathbf{g_k}(t)||^2}\right)^+, (E_k(t) - P_c)^+\right]. \tag{27}$$

Proof: Due to the space limit, the detailed proof can be found in Appendix D in https://www.researchgate.net/publication/329527135_Buffer-aided_Adaptive_Wireless_Powered_Communication_Network_with_Finite_Energy_Storage_and_Data_Buffer [34]. ∎

It is worth noting that, unlike the traditional scheme, now the power allocation scheme is not only related to the current channel state, but also depends on the current virtual energy queue and virtual data queue. With the increase in $\tilde{Q}_k$ and $\tilde{E}_k$, the transmit power of the corresponding user U_k will be larger. It is very interesting that at most one user is scheduled for transmission in each time slot. That is, with the help of the data buffer and the energy buffer, the time resource is always assigned to the user who has a larger data queue, larger energy queue or better channel state in that time slot.

F. Transmission Mode Selection

When the optimal energy beamforming, the power and time allocation scheme in the corresponding mode have been obtained, by substituting them into the objective function of the corresponding optimization problem, we can obtain the optimal transmission mode selection scheme as follows

$$d(t)=\begin{cases}0, & \text{if } \mathcal{M}_1(t)\le \mathcal{M}_2(t),\\ 1, & \text{otherwise,}\end{cases} \tag{28}$$

where

$$\mathcal{M}_1(t)=-\sum_{k=1}^{K}\mu_{2k}(\phi_k-\tilde{E}_k(t))|\mathbf{g_k}(\mathbf{t})\mathbf{w}(\mathbf{t})|^2\zeta+Z(t)||\mathbf{w}(\mathbf{t})||^2, \tag{29}$$

$$\mathcal{M}_2(t)=\sum_{k=1}^{K}\Bigg[-\mu_{1k}\tilde{Q}_k(t)\tau_k(t)\log_2\left(1+\frac{P_k(t)||\mathbf{g_k}(\mathbf{t})||^2}{\sigma^2}\right)+\mu_{2k}(\phi_k-\tilde{E}_k(t))C_k(t)\tau_k(t)\Bigg]. \tag{30}$$

From the transmission mode selection scheme, we may observe that, the RF energy transmission mode will be selected when there is a smaller energy queue size $\tilde{E}_k(t)$. With the increase in energy queue size $\tilde{E}_k(t)$ and data queue size $\tilde{Q}_k(t)$ (more data awaiting for transmission), the system tends to activate the data transmission mode. In the data transmission mode, the energy queue size $\tilde{E}_k(t)$ and the data queue size $\tilde{Q}_k(t)$ will be decreased until the system goes back to the RF energy transmission mode. In this way, the queue stability of the virtual data queues and virtual energy queues can be ensured by using the proposed transmission scheme.

G. Performance Analysis

Theorem 1: When the proposed rate control, energy beamforming, time allocations, power allocations, and mode selection algorithms are used, for any $V>0$, the average virtual queue size, QoS constraints, and the long-term weighted sum-rate fulfill the following constraints:

$$\tilde{Q}_k(t)\le\frac{\theta_k V}{\mu_{1k}(1-\eta_d^k)}+(1-\eta_d^k)\hat{A}_k, \tag{31}$$

$$(\phi_k-\tilde{E}_k(t))\le\frac{\mu_{1k}\hat{g}_k}{\mu_{2k}\sigma^2}\left(\frac{\theta_k V}{\mu_{1k}(1-\eta_d^k)}+(1-\eta_d^k)\hat{A}_k\right)+\hat{C}_k+N_h^k\xi, \tag{32}$$

$$Z(t)\le\frac{1}{\mu_3}\sum_{k=1}^{K}\left(\frac{\mu_{1k}\hat{g}_k}{\sigma^2}\left(\frac{\theta_k V}{\mu_{1k}(1-\eta_d^k)}+(1-\eta_d^k)\hat{A}_k\right)+\mu_{2k}\hat{C}_k+\mu_{2k}N_h^k\xi\right)\hat{g}_k\zeta+P_{\max}, \tag{33}$$

$$P_{loss}^k\le\eta_d^k, \tag{34}$$

$$P_0^k\le\eta_0^k, \tag{35}$$

$$\limsup_{t\to\infty}\frac{1}{T}\sum_{t=0}^{T-1}(1-d(t))||\mathbf{w}(t)||^2\le\bar{P}_{\max}, \tag{36}$$

$$\liminf_{T\to\infty}\frac{1}{T}\sum_{t=0}^{T-1}\sum_{k=1}^{K}\theta_k a_k(t)\ge\liminf_{T\to\infty}\frac{1}{T}\sum_{t=0}^{T-1}\sum_{k=1}^{K}\theta_k a_k^*(t)-\sum_{k=1}^{K}\frac{\theta_k\eta_0^k}{1-\eta_d^k}\left(\hat{R}_k+\frac{\hat{g}_k\xi}{\sigma^2}\right)-O\left(\frac{1}{V}\right)-\sum_{k=1}^{K}O\left(\frac{(\frac{\theta_k V}{1-\eta_d^k}-\mu_{1k}\hat{Q}_k)^+}{V}\right)-\sum_{k=1}^{K}O\left(\frac{(\frac{\theta_k\hat{g}_k V}{(1-\eta_d^k)\sigma^2}-\mu_{2k}\hat{E}_k)^+}{V}\right), \tag{37}$$

where $a_k^*(t)$ is the theoretically optimal rate at which data are placed in B_{dk}, and N_h^k is the maximum number of time slots required when the energy state of U_k changes from 0 to E_k^{re}.

Proof: Due to the space limit, the detailed proof can be found in Appendix E in https://www.researchgate.net/publication/329527135_Buffer-aided_Adaptive_Wireless_Powered_Communication_Network_with_Finite_Energy_Storage_and_Data_Buffer [34]. ■

From ***Theorem 1***, we may notice that the virtual queue length of $\tilde{Q}_k(t)$, $(\phi_k-\tilde{E}_k(t))$ and $Z(t)$ grows linearly with V. The proposed scheme can effectively ensure that the constraints on data buffer, energy storage, and the average power consumption can be satisfied. (37) explicitly shows the achieved long-term weighted sum-rate performance lower bound. The term $\sum_{k=1}^{K}\frac{\theta_k\eta_0^k}{1-\eta_d^k}\left(\hat{R}_k+\frac{\hat{g}_k}{\sigma^2}\right)$ corresponds to the loss owing to the data loss ratio and the case when energy buffer is below E_k^{re}. The maximally allowed frequency η_0^k of energy state $E_k(t)$ below E_k^{re} should be set to be small enough to guarantee the other normal tasks of U_k. The loss item of $\sum_{k=1}^{K}O\left(\frac{(\frac{\theta_k V}{1-\eta_d^k}-\mu_{1k}\hat{Q}_k)^+}{V}\right)$ and $\sum_{k=1}^{K}O\left(\frac{(\frac{\theta_k\hat{g}_k V}{(1-\eta_d^k)\sigma^2}-\mu_{2k}\hat{E}_k)^+}{V}\right)$ corresponds to the influence by finite data buffer size and energy storage size, respectively. If the size of data buffer and energy buffer are large enough and η_0^k is set to be very small, the loss items tend to be diminished, and the gap between the proposed scheme and the optimal one in terms of the long-term sum rate is inversely proportional to V.

V. Weighted Max-Min Fair Access Design

Note that the maximized weighted sum-rate solution in Section IV may lead to an unfairness problem due to the near-far issue. In this section, in order to guarantee the access fairness among different terminals in the WPCN, we propose the weighted max-min fair access design, which can ensure that the data rate of all participating terminals are weighted max-min fair. And the weighted max-min fair access design problem can be formulated as below

$$(\mathcal{P}\mathbf{3}):\max_{\mathbf{w}(\mathbf{t}),P_k(t),a_k(t),\tau_k(t),d(t)}\liminf_{T\to\infty}\frac{1}{T}\min\Big[\frac{1}{\theta_1}\sum_{t=0}^{T-1}a_1(t),\frac{1}{\theta_2}\sum_{t=0}^{T-1}a_2(t),\ldots,\frac{1}{\theta_K}\sum_{t=0}^{T-1}a_K(t)\Big]$$
$$\text{s.t. } C1\sim C11, \tag{38}$$

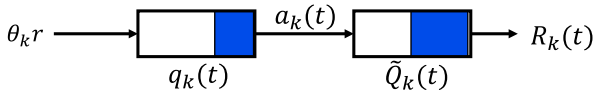

Fig. 5. The relationship between the virtual queue $q_k(t)$ and $\tilde{Q}_k(t)$.

where $\theta_k > 0$ $(k = 1, 2, \ldots, K)$ are weighting coefficients. The value of θ_k stands for the priority or weight of U_k, and a larger θ_k implies that U_k has a higher priority. To solve the above optimization problem, we introduce a new auxiliary variable

$$r = \liminf_{T\to\infty} \frac{1}{T} \min \Bigg\{ \frac{1}{\theta_1} \sum_{t=0}^{T-1} a_1(t), \frac{1}{\theta_2} \sum_{t=0}^{T-1} a_2(t), \ldots, \frac{1}{\theta_K} \sum_{t=0}^{T-1} a_K(t) \Bigg\}, \quad (39)$$

so the optimization problem $\mathcal{P}\mathbf{3}$ can be transformed into an equivalent problem as follows

$$\begin{aligned} \max_{\mathbf{w}(\mathbf{t}), P_k(t), a_k(t), \tau_k(t), d(t)} \quad & r \\ \text{s.t.} \quad & r \le \liminf_{T\to\infty} \frac{1}{T} \frac{1}{\theta_k} \sum_{t=0}^{T-1} a_k(t), \quad k = 1, 2, \ldots K, \\ & C1 \sim C11. \end{aligned} \quad (40)$$

To ensure that the constraint $r \le \liminf_{T\to\infty} \frac{1}{T\theta_k} \sum_{t=0}^{T-1} a_k(t)$ is satisfied, we define the following virtual queue

$$q_k(t+1) = \big(q_k(t) + \theta_k r - a_k(t)\big)^+, \quad k = 1, 2, \cdots, K. \quad (41)$$

If the virtual queue $q_k(t)$ is rate stable, we can get $r \le \liminf_{T\to\infty} \frac{1}{T\theta_k} \sum_{t=0}^{T-1} a_k(t)$. The proof is similar to that in Appendix A, so we omit it here to save space. In Fig. 5 we show the relationship between the virtual queue $q_k(t)$ and $\tilde{Q}_k(t)$, where the output of $q_k(t)$ is the input of $\tilde{Q}_k(t)$, which can be regarded as a serial system. When all the virtual queues are stable, the optimal scheduling will make the average input of the system equal to the average output. The input of virtual queue $q_k(t), k = 1, 2, \cdots, K$ in each time slot is $\theta_k r$, which will lead to $\liminf_{T\to\infty} \frac{1}{T\theta_1} \sum_{t=0}^{T-1} R_1(t) = \cdots = \liminf_{T\to\infty} \frac{1}{T\theta_K} \sum_{t=0}^{T-1} R_K(t) = r$, and thus the weighted max-min fairness of users will be satisfied. Similarly, the Lyapunov optimization framework can be utilized to transform the optimization problem as below

$$\begin{aligned} \min_{\mathbf{w}, P_k, a_k, \tau_k, d} \quad & \sum_{k=1}^{K} \Big\{ \mu_{1k} \tilde{Q}_k(t) \big((1 - \eta_d^k) a_k(t) - R_k(t) \big) \\ & + \mu_{2k} (\phi_k - \tilde{E}_k(t)) \big(- H_k(t) + C_k(t) \big) \Big\}, \\ & + \mu_3 Z(t) (1 - d(t)) ||\mathbf{w}(\mathbf{t})||^2 \\ & + \sum_{k=1}^{K} \mu_{4k} q_k(t) \big(\theta_k r - a_k(t) \big) - Vr, \\ \text{s.t.} \quad & C3 \sim C5, C9 \sim C11, \end{aligned} \quad (42)$$

where $\mu_{4k}, k = 1, \cdots, K$, is a nonnegative constant. Obviously, the optimal energy beamforming design, time and power allocations, and mode selection are consistent with the long-term average weighted sum-rate maximization problem, and the only difference is the rate control problem. The rate control problem can be simplified as follows

$$\begin{aligned} \min_{r, a_k(t)} \quad & \sum_{k=1}^{K} \big(\mu_{1k} \tilde{Q}_k(t) (1 - \eta_d^k) - \mu_{4k} q_k(t) \big) a_k(t) \\ & + \Big(\sum_{k=1}^{K} \mu_{4k} q_k(t) \theta_k - V \Big) r \\ \text{s.t.} \quad & 0 \le a_k(t) \le A_k(t), \quad k = 1, 2, \cdots, K. \end{aligned} \quad (43)$$

The objective function and constraint conditions are linear with respect to the optimization variables, and thus the optimal rate control scheme is given by

$$a_k(t) = \begin{cases} A_k(t), & \text{if } \mu_{4k} q_k(t) \ge \mu_{1k} \tilde{Q}_k(t) (1 - \eta_d^k), \\ 0, & \text{otherwise.} \end{cases} \quad (44)$$

In each time slot, r is updated as below

$$r = \begin{cases} 0, & \\ & \text{if } V < \sum_{k=1}^{K} \mu_{4k} q_k(t) \theta_k, \\ a_{\min}(t) + \lambda(t) \big(\bar{a}(t) - a_{\min}(t) \big), & \\ & \text{othetwise,} \end{cases} \quad (45)$$

where $a_{\min}(t) = \frac{1}{t} \min \big[\frac{1}{\theta_1} \sum_{i=0}^{t-1} a_1(i), \ldots, \frac{1}{\theta_K} \sum_{i=0}^{t-1} a_K(i) \big]$, $\bar{a}(t) = \frac{1}{Kt} \sum_{k=1}^{K} \sum_{i=0}^{t-1} \frac{1}{\theta_k} a_k(i)$ and $\lambda(t)$ is the utilized step at time t. Here, we use the idea of greedy algorithm to make $a_{\min}(t)$ approach $\bar{a}(t)$ as close as possible, which will gradually increase $a_{\min}(t)$ until $a_{\min}(t) = \bar{a}(t)$.

VI. Numerical Analysis

In this section, we evaluate the performance of the proposed buffer-aided adaptive wireless powered communication network through Monte-Carlo simulations. The size of the data buffer B_{dk} and the size of the energy buffer B_{ek} are assumed to be $\hat{Q}_k = 1000$Mbit and $\hat{E}_k = 1$J, respectively. The bandwidth is set to be 1MHz. The path loss exponent $m = 2$, and thus the channel power gain from the AP to U_k is modeled as $\mathbf{g_k(t)} = \sqrt{10^{-3} d_k^{-m}} \mathbf{g_k^{an}}$ with $\mathbf{g_k^{an}} = [\rho_{1,k}(t)\ \rho_{2,k}(t) e^{j\vartheta_k}\ \ldots\ \rho_{N,k}(t) e^{j(N-1)\vartheta_k}]$, where d_k denotes the distance between the AP and U_k, $\rho_{i,k}(t)$ denotes the additional channel short-term fading from the i-th antenna of the AP to U_k, which is assumed to follow Rayleigh distribution with unit fading power gain. Thus, $\rho_{i,k}^2(t)$ is an exponential distributed random variable with unit mean, $\vartheta_k = -\frac{2\pi d^{an} \sin(\varphi_k)}{\lambda}$, d^{an} is the spacing between successive antenna elements at the AP, λ is the wavelength of RF energy signal, and φ_k is the direction of U_k to the AP. We assume that there is about 30dB average signal power attenuation at a reference distance of 1m. The noise at all nodes are assumed to have a white power spectral density of -160dBm/Hz. The energy conversation efficiency is assumed to be $\zeta = 0.5$. The arrival rate $A_k(t), k = 1, \cdots, K$ is modeled as Poisson random variable with mean $\Omega_k = 15$ Mbps. Unless otherwise stated, we assume that the AP is equipped with $N = 4$ antennas, there are two users, the distance from users to the AP

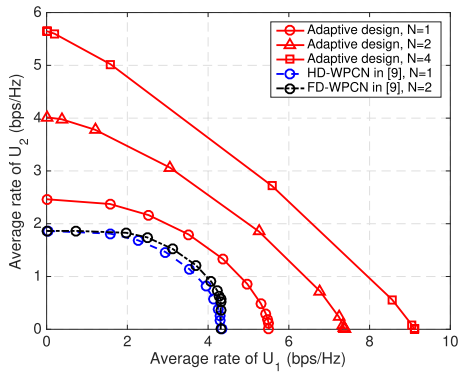

Fig. 6. Average achievable rate region with $\bar{P}_{\max} = 10$dBm.

are $d_1 = 5$ m and $d_2 = 10$ m, $d^{an} = \frac{\lambda}{2}$, $\{\varphi_1, \varphi_2\} = \{0°, 45°\}$, the circuit power consumption of terminals is $P_c = 0$ μW, the weighting coefficients in the weighted max-min fair access design are assumed to be $\theta_1 = \theta_2 = 1$, the initial energy state is $E_k(0) = 0.1$ J, the maximal transmit power of the AP is $P_{\max} = 5\bar{P}_{\max}$, the maximal virtual energy queue is $\phi_k = \bar{P}_{\max}$, and the weighted values are $\mu_{1k} = 10^4\bar{P}_{\max}$, $\mu_{2k} = 2 \times 10^{11}/\phi_k$, $\mu_3 = 10^2$, and $\mu_{4k} = 10^2\bar{P}_{\max}$. We assume that each terminal needs to reserve 0.1 J of energy to meet other tasks, *i.e.*, $E_k^{re} = 0.1$ J. We set the long-term data loss ratio $\eta_d^k = 0$ and the frequency of the energy state is below E_k^{re} is $\eta_0^k = 0$ such that the normal operation of terminals can be ensured. All the presented simulation results are obtained for $T = 10^6$ slots.

To evaluate the performance of the proposed transmission scheme for the wireless powered communication network, we consider HD-WPCN and FD-WPCN with perfect self-interference cancellation schemes proposed in [9] as the benchmark schemes, where the terminal has neither data buffer nor energy buffer. For the FD-WPCN scheme in [9], the AP is equipped with two antennas, one of which is used to broadcast energy and the other one is used to receive user information simultaneously. Fig. 6 presents the average achievable rate region of the proposed adaptive design and the benchmark scheme. One may observe that the average rate region of the proposed adaptive design is always superior to the benchmark schemes. Even when the AP is only equipped with a single antenna, the performance of the proposed adaptive design is noticeably superior to the FD-WPCN scheme. As the number of antennas increases, the average rate region will gradually increase, which can be explicated by the spatial gain owing to multiple antenna utilized at AP. Fig. 7 illustrates the long-term average sum-rate and the individual throughput of the proposed adaptive design versus the average power consumption. For comparison, the benchmark schemes are included as well. We may notice that, when the AP is equipped with a single antenna, the proposed adaptive design can increase the sum-rate by 13% to 30% when compared with the HD-WPCN scheme. When the AP is equipped with two antennas, the average sum rate of the proposed adaptive design can be improved by 21% to 88% when compared with the FD-WPCN scheme. However, the average rate of U_1 dominates over that of U_2 due

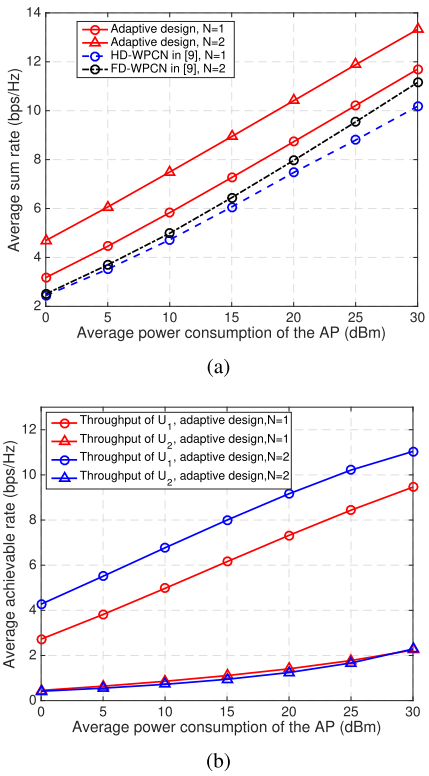

Fig. 7. The achieved long-term average rate of the proposed adaptive design; (a) sum-rate, and (b) individual throughput.

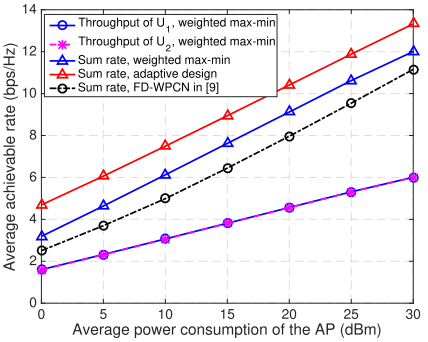

Fig. 8. The achieved long-term average sum-rate and individual throughput of the proposed max-min fair access design, $N = 2$.

to U_1 is closer to the AP, which leads to the notably unfair rate allocation between the near user U_1 and far user U_2. As the number of antennas increases, the unfairness between U_1 and U_2 becomes even more notable. This is because the energy beam is mainly directed to the closer user U_1 such that the sum rate can be effectively increased.

Fig. 8 shows the long-term average sum rate of the proposed weighted max-min fair access design versus the average power consumption. And the proposed adaptive design with $\theta_k = 0.5$, $k = 1, 2$ and the FD-WPCN scheme in [9] are included for comparison. Now it is observed that the average achievable rates of U_1 and U_2 are very close to each other, which implies that the proposed weighted max-min fair access design can effectively guarantee the fair access requirements by different terminals. Although the paid cost of the max-min

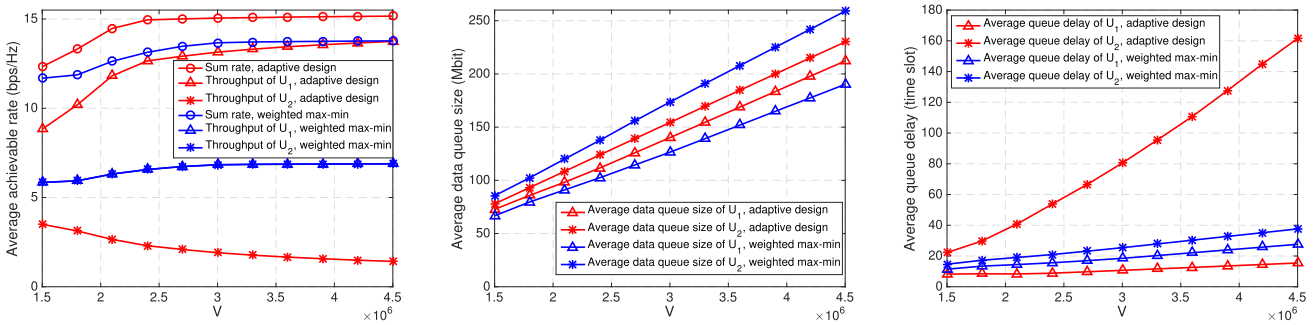

Fig. 9. Average achievable rate, queue size, and delay with different choice of V with $\bar{P}_{\max} = 30$dBm; (a) average achievable rate, (b) average queue size, and (c) average queue delay.

fair access design compared to the adaptive design is some loss in the achieved sum rate, the average achievable sum rate can also be noticeably improved when compared with the FD-WPCN scheme in [9].

Next, by fixing $\bar{P}_{\max} = 30$dBm, the impact of different choice V on the achieved performance are shown in Fig. 9. We may notice from Fig. 9(a) that, in the proposed adaptive design, the achievable rate of U_1 gradually increases with the increase in V. However, the achievable rate of U_2 will gradually decrease as V increases. This is because the system has to allocate more time resources to near user U_1, and the energy beams are also mainly directed to near user U_1 in order to further improve the sum rate. By employing the proposed weighted max-min fair access design, now both users will have almost the same achievable rate, which will increase with the increase in V until a stable sum rate value. As expected, the sum rate of the proposed weighted max-min fair access design is also inferior to the sum rate of the proposed adaptive design, which complies with the results in Fig. 8. The relationship between the average queue size and the data transmission delay versus the choice of V is illustrated in Fig. 9(b) and Fig. 9(c), respectively. One may observe that, as expected, the average queue size are proportional to V, and the average queue delay gradually increases as V increases. It is worth noting that, the far user U_2 always has a larger average queue and delay. And this can be explicated by the fact that, the far user U_2 has a worse channel, which leads to a larger queue backlog, and a large average queue size and delay accordingly. By comparing with Fig. 9(a), one may readily conclude that, larger achievable rates can be realized if a larger transmission delay is tolerable.

The impact of different choice of V on average time allocation for data transmission mode and energy harvesting mode are illustrated in Fig.10. It can be observed that, the time allocated for energy harvesting gradually decreases with the increase in V until to approach some stable value. And it can be noted that, more time will be allocated to energy harvesting mode in the weighted max-min fair design than the adaptive design. This is because far user U_2 needs more energy harvesting to achieve the almost the same transmission rate as the near user U_1. And the time allocation for two users in data transmission mode also clearly shows us the difference

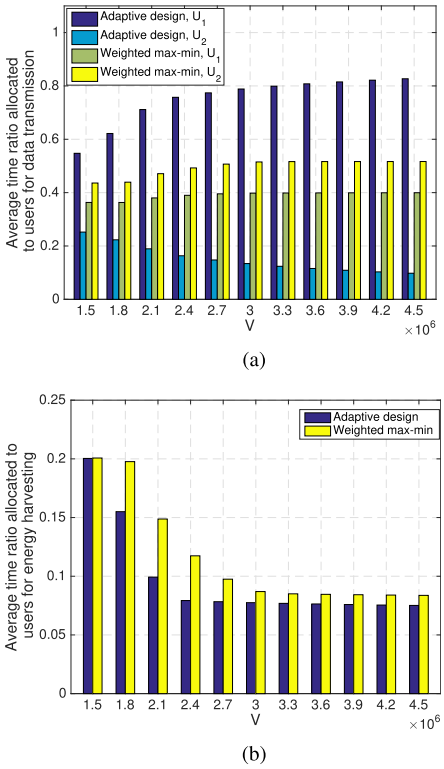

Fig. 10. Average time allocation with different choice of V with $\bar{P}_{\max} = 30$dBm; (a) time allocation for data transmission, and (b) time allocation for energy harvesting.

in between the adaptive design and the weighted max-min fair access design. In the adaptive design, more time resource will be allocated to the near user U_1 to further improve the sum rates with the increase in V. Nonetheless, in the weighted max-min fair access design more time resources will be allocated to the far user U_2 such that the fairness can be ensured, which complies with the results in Fig. 9(a).

In Fig. 11 we illustrate the average achievable rate with different weighting choices in the weighted max-min fair access design. We can observe that, the average achievable rate of U_i (U_j), $i, j = 1, 2, i \neq j$ increases (decreases) as the weighting coefficient θ increases when $\theta_i = \theta$ and $\theta_j = 1$. Moreover, the average achievable rate of U_j is very close to

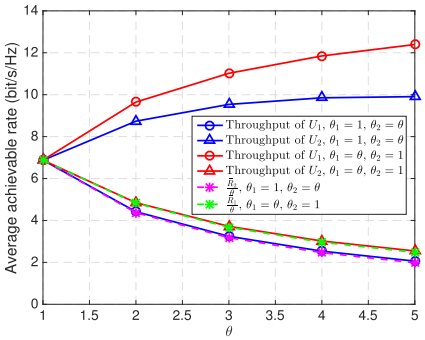

Fig. 11. Average achievable rate with different weighting choices in the weighted max-min fair access design when $\bar{P}_{\max} = 30$ dBm.

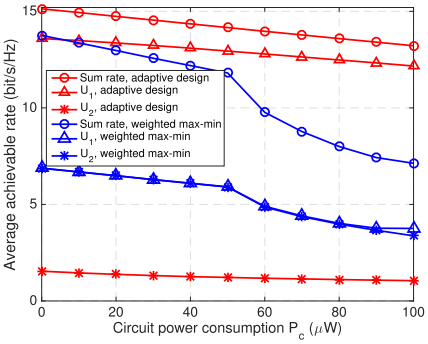

Fig. 12. The impact of circuit power consumption on the average achievable rate in the buffer-aided adaptive design and the weighted max-min design when $N = 4$ and $\bar{P}_{\max} = 30$ dBm.

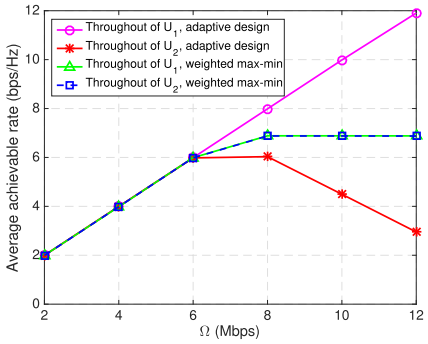

Fig. 13. The impact of the average arrival rates on the average achievable rate with $\Omega_1 = \Omega_2 = \Omega$.

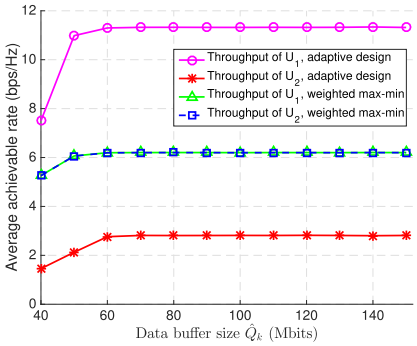

Fig. 14. The impact of different data buffer size $\hat{Q}_k$ on average achievable rate with $V = 2 \times 10^6$.

the average achievable rate of U_i divided by θ. Likewise, we will have similar average achievable rate performance when $\theta_i = 1$ and $\theta_j = \theta$. These simulation results confirm that, the proposed weighted max-min fair access design can effectively guarantee the priority of different users by properly setting the predetermined weighting coefficient.

Fig. 12 presents the impact of circuit power consumption on the average achievable rate in the proposed buffer-aided adaptive design and the weighted max-min fair access design. It can be observed that the achievable rate will decrease with the increase in circuit power consumption. Moreover, compared with the adaptive design, the weighted max-min fair access design is more susceptible to circuit power consumption. This is because, in order to guarantee fairness among users, the weighted max-min access design has to allocate more time resources to the far away user U_2 for data transmission, which gives rise more energy consumption at U_2 in circuit operation than that with the adaptive design.

The relationship between the average achievable rate and the average arrival rates in the proposed scheme are shown in Fig. 13. When the arrival rate is within the capacity region, the transmission rate by users can be effectively satisfied. When the arrival rate exceeds the maximum rate that the system can support, the adaptive design will give priority to meeting the requirements by the near user U_1, while the max-min fair access design will try to ensure the fairness of both users, as expected. Fig. 14 shows the relationship between the achievable rate and the different data buffer size $\hat{Q}_k$. We can see that, as $\hat{Q}_k$ increases, the achievable rate gradually increases until a stable value, and then as the data buffer continues to increase, the achievable rate will not increase. This can be interpreted in this way that, the larger $\hat{Q}_k$ implies that a larger data rate from the upper layer is tolerable. The stable achievable rate corresponds to the available resource limits.

The impact of different η_0^k and η_d^k on system performance are presented in Fig. 15. We may notice that the actual long-term data loss ratio and the frequency of the energy state below E_k^{re} are always less than the given threshold η_d^k and η_0^k, respectively. It indicates that the proposed adaptive design and the max-min fair access design can effectively ensure the constraints on data buffer and energy storage. The sum rate of the adaptive design and max-min fair access design increase as η_d^k increases. This can be explicated by the fact that, a larger η_d^k implies a higher frequency of data buffer is sufficiently filled, which requires more time slots for data transmission to ensure the data queues are stable. Hence there will be some performance improvement in the sum rate. Besides, the sum rate will increase as η_0^k increases until a stable value. This can be explained by the fact that, when $\eta_0^k = 0$, the users have to spend more time on harvesting energy to ensure the energy states are always larger than the given desired value at any time slot, hence there will be some loss in the sum rate when $\eta_0^k = 0$.

Fig. 16 presents the impact of the path loss exponent on the average achievable rate over Rician fading channel

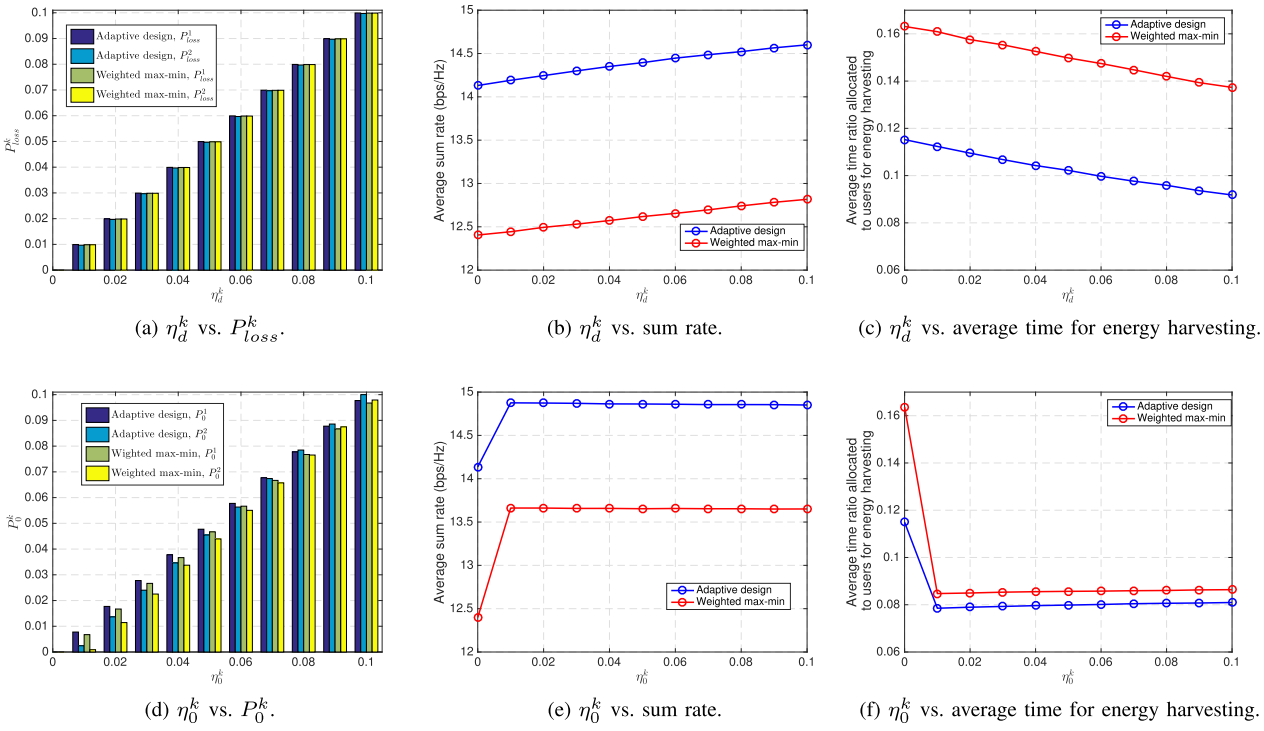

(a) η_d^k vs. P_{loss}^k. (b) η_d^k vs. sum rate. (c) η_d^k vs. average time for energy harvesting.

(d) η_0^k vs. P_0^k. (e) η_0^k vs. sum rate. (f) η_0^k vs. average time for energy harvesting.

Fig. 15. The impact of different η_0^k and η_d^k on system performance with $\bar{P}_{\max} = 30$dBm and $V = 2 \times 10^6$.

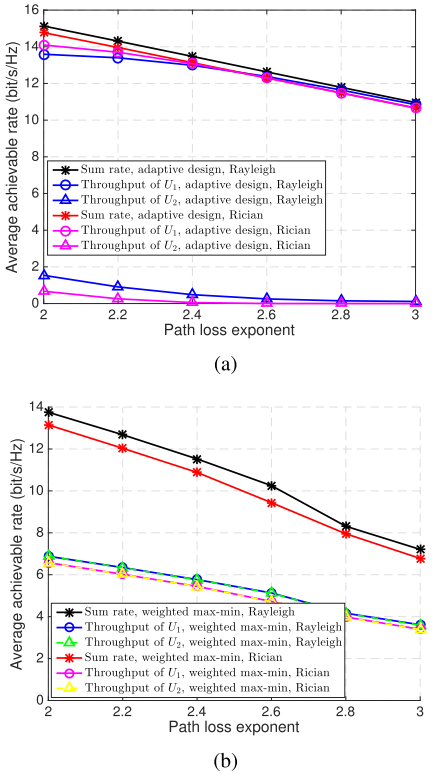

(a)

(b)

Fig. 16. The impact of the path loss exponent on the average achievable rate when the Rician factor is 10 dB; (a) adaptive design, and (b) weighted max-min fair access design.

and Rayleigh fading channel. To ensure a fair comparison, the channel power gains of both the Rayleigh fading channel and the Rician channels are normalized to be unit. We can observe that, as expected, the average achievable rate decreases with the increase in the path loss exponent. Interestingly, both the proposed adaptive design and the proposed weighted max-min fair access design can realize larger average achievable rates over the Rayleigh fading channel than those over the Rician fading channel. This is because the Rician fading channel comprises of the line-of-sight component, which makes the channel tend to be more stable than the Rayleigh fading channel. And less variations in the channel quality over the Rician fading channel will decrease the probability that the user channel is in relative good conditions, thereby reducing the multiuser scheduling gain in the proposed design. Furthermore, the proposed weighted max-min fair access design can effectively ensure average achievable rates of different users are almost the same under over both the Rician fading and the Rayleigh fading channels. This indicates that the proposed algorithm can be applied to various wireless channels.

VII. Conclusion

In this paper, we consider a realistic WPCN, where every individual wireless terminal is equipped with a finite energy storage and a finite data buffer. First, in order to maximize the sum rate of the whole system, the energy beamforming, the optimal power allocations, rate control, time allocations, and the transmission mode selection have been jointly considered in the proposed adaptive design to maximize the long-term average weighted sum-rate. However, in the presence of the heterogenous link qualities, the sum rate maximization by the proposed adaptive design tends to allocate more resources to users with favorable channel conditions, which gives rise to unfair access issue. In order to ensure the fair access

requirements, a weighted max-min fair access design was proposed. It is shown that, the proposed adaptive design can fully exploit the temporal diversity gains, while the weighted max-min fair access design can effectively ensure the fair access requirements by different users with some loss in the achieved sum-rate. In addition, an inherent tradeoff between transmission rate and average queue delay is disclosed to show that, the higher transmission rate can be achieved if a larger delay is tolerable. Simulation results showed that the proposed adaptive design can significantly improve the average achievable rate region compared to HD-WPCN and FD-WPCN scheme, although there is some loss in the achieved sum rate performance, the proposed weighted max-min fair access design still noticeably outperforms the FD-WPCN scheme when ensuring the fair access requirements by participating terminals.

REFERENCES

[1] Q. Wu, G. Y. Li, W. Chen, D. W. K. Ng, and R. Schober, "An overview of sustainable green 5G networks," *IEEE Wireless Commun.*, vol. 24, no. 4, pp. 72–80, Aug. 2017.

[2] X. Zhou, R. Zhang, and C. K. Ho, "Wireless information and power transfer: Architecture design and rate-energy tradeoff," *IEEE Trans. Commun.*, vol. 61, no. 11, pp. 4754–4767, Nov. 2013.

[3] A. A. Nasir, X. Zhou, S. Durrani, and R. A. Kennedy, "Relaying protocols for wireless energy harvesting and information processing," *IEEE Trans. Wireless Commun.*, vol. 12, no. 7, pp. 3622–3636, Jul. 2013.

[4] R. Zhang and C. K. Ho, "MIMO broadcasting for simultaneous wireless information and power transfer," *IEEE Trans. Wireless Commun.*, vol. 12, no. 5, pp. 1989–2001, May 2013.

[5] E. Boshkovska, D. W. K. Ng, N. Zlatanov, and R. Schober, "Practical non-linear energy harvesting model and resource allocation for SWIPT systems," *IEEE Commun. Lett.*, vol. 19, no. 12, pp. 2082–2085, Dec. 2015.

[6] M.-M. Zhao *et al.*, "Robust transceiver design for MISO interference channel with energy harvesting," *IEEE Trans. Signal Process.*, vol. 64, no. 17, pp. 4618–4633, Sep. 2016.

[7] Q. Shi, L. Liu, W. Xu, and R. Zhang, "Joint transmit beamforming and receive power splitting for MISO SWIPT systems," *IEEE Trans. Wireless Commun.*, vol. 13, no. 6, pp. 3269–3280, Jun. 2014.

[8] H. Ju and R. Zhang, "Throughput maximization in wireless powered communication networks," *IEEE Trans. Wireless Commun.*, vol. 13, no. 1, pp. 418–428, Jan. 2014.

[9] H. Ju and R. Zhang, "Optimal resource allocation in full-duplex wireless-powered communication network," *IEEE Trans. Commun.*, vol. 62, no. 10, pp. 3528–3540, Oct. 2014.

[10] L. Liu, R. Zhang, and K.-C. Chua, "Multi-antenna wireless powered communication with energy beamforming," *IEEE Trans. Commun.*, vol. 62, no. 12, pp. 4349–4361, Dec. 2014.

[11] X. Kang, C. K. Ho, and S. Sun, "Full-duplex wireless-powered communication network with energy causality," *IEEE Trans. Wireless Commun.*, vol. 14, no. 10, pp. 5539–5551, Oct. 2015.

[12] H. Ju and R. Zhang, "User cooperation in wireless powered communication networks," in *Proc. IEEE GLOBECOM*, Dec. 2014, pp. 1430–1435.

[13] X. Di, K. Xiong, P. Fan, H.-C. Yang, and K. B. Letaief, "Optimal resource allocation in wireless powered communication networks with user cooperation," *IEEE Trans. Wireless Commun.*, vol. 16, no. 12, pp. 7936–7949, Dec. 2017. doi: 10.1109/TWC.2017.2754494.

[14] Z. Chu, F. Zhou, Z. Zhu, M. Sun, and N. Al-Dhahir, "Energy beamforming design and user cooperation for wireless powered communication networks," *IEEE Wireless Commun. Lett.*, vol. 6, no. 6, pp. 750–753, Dec. 2017. doi: 10.1109/LWC.2017.2739148.

[15] H. Lee, K.-J. Lee, H. Kim, B. Clercks, and I. Lee, "Resource allocation techniques for wireless powered communication networks with energy storage constraint," *IEEE Trans. Wireless Commun.*, vol. 15, no. 4, pp. 2619–2628, Apr. 2016.

[16] K. W. Choi and D. I. Kim, "Stochastic optimal control for wireless powered communication networks," *IEEE Trans. Wireless Commun.*, vol. 15, no. 1, pp. 686–698, Jan. 2016.

[17] J. Yang, Q. Yang, K. S. Kwak, and R. R. Rao, "Power–delay tradeoff in wireless powered communication networks," *IEEE Trans. Veh. Technol.*, vol. 66, no. 4, pp. 3280–3292, Apr. 2017.

[18] Z. Hadzi-Velkov, I. Nikoloska, H. Chingoska, and N. Zlatanov, "Opportunistic scheduling in wireless powered communication networks," *IEEE Trans. Wireless Commun.*, vol. 16, no. 6, pp. 4106–4119, Jun. 2017.

[19] S. Bi, Y. Zeng, and R. Zhang, "Wireless powered communication networks: An overview," *IEEE Wireless Commun.*, vol. 23, no. 2, pp. 10–18, Apr. 2016.

[20] R. A. Berry and R. G. Gallager, "Communication over fading channels with delay constraints," *IEEE Trans. Inf. Theory*, vol. 48, no. 5, pp. 1135–1149, May 2002.

[21] B. Xia, Y. Fan, J. Thompson, and H. V. Poor, "Buffering in a three-node relay network," *IEEE Trans. Wireless Commun.*, vol. 7, no. 11, pp. 4492–4496, Nov. 2008.

[22] N. Zlatanov, R. Schober, and P. Popovski, "Buffer-aided relaying with adaptive link selection," *IEEE J. Sel. Areas Commun.*, vol. 31, no. 8, pp. 1530–1542, Aug. 2013.

[23] Y. Liu, Q. Chen, X. Tang, and L. X. Cai, "On the buffer energy aware adaptive relaying in multiple relay network," *IEEE Trans. Wireless Commun.*, vol. 16, no. 9, pp. 6248–6263, Sep. 2017.

[24] X. Lan, Q. Chen, X. Tang, and L. Cai, "Achievable rate region of the buffer-aided two-way energy harvesting relay network," *IEEE Trans. Veh. Technol.*, vol. 67, no. 11, pp. 11127–11142, Nov. 2018.

[25] A. Ikhlef, D. S. Michalopoulos, and R. Schober, "Max-max relay selection for relays with buffers," *IEEE Trans. Wireless Commun.*, vol. 11, no. 3, pp. 1124–1135, Mar. 2012.

[26] N. Zlatanov, A. Ikhlef, T. Islam, and R. Schober, "Buffer-aided cooperative communications: Opportunities and challenges," *IEEE Commun. Mag.*, vol. 52, no. 4, pp. 146–153, Apr. 2014.

[27] Y. Liu, Q. Chen, and X. Tang, "On the adaptive transmission scheme in buffer-aided wireless powered relay network," in *Proc. IEEE GLOBECOM*, Dec. 2016, pp. 1–6.

[28] B. Varan and A. Yener, "Energy harvesting two-way communications with limited energy and data storage," in *Proc. 48th Asilomar Conf. Signals, Syst. Comput.*, Nov. 2014, pp. 1671–1675.

[29] Z. Mao, C. E. Koksal, and N. B. Shroff, "Near optimal power and rate control of multi-hop sensor networks with energy replenishment: Basic limitations with finite energy and data storage," *IEEE Trans. Autom. Control*, vol. 57, no. 4, pp. 815–829, Aug. 2012.

[30] V. Jamali, N. Zlatanov, A. Ikhlef, and R. Schober, "Achievable rate region of the bidirectional buffer-aided relay channel with block fading," *IEEE Trans. Inf. Theory*, vol. 60, no. 11, pp. 7090–7111, Nov. 2014.

[31] Y. Liu, Q. Chen, and X. Tang, "Adaptive buffer-aided wireless powered relay communication with energy storage," *IEEE Trans. Green Commun. Netw.*, vol. 2, no. 2, pp. 432–445, Jun. 2018.

[32] Q. Wu, M. Tao, D. W. K. Ng, W. Chen, and R. Schober, "Energy-efficient resource allocation for wireless powered communication networks," *IEEE Trans. Wireless Commun.*, vol. 15, no. 3, pp. 2312–2327, Mar. 2016.

[33] Q. Wu, W. Chen, D. W. K. Ng, and R. Schober, "Spectral and energy-efficient wireless powered IoT networks: NOMA or TDMA?" *IEEE Trans. Veh. Technol.*, vol. 67, no. 7, pp. 6663–6667, Jul. 2018.

[34] X. Lan and Q. Chen. *Buffer-Aided Adaptive Wireless Powered Communication Network With Finite Energy Storage and Data Buffer*. Accessed: Dec. 2018. [Online]. Available: https://www.researchgate.net/publication/329527135_Buffer-aided_Adaptive_Wireless_Powered_Communication_Network_with_Finite_Energy_Storage_and_Data_Buffer

Xiaolong Lan received the B.E. degree in mathematics and applied mathematics from the Chengdu University of Technology, China, in 2012. He is currently pursuing the Ph.D. degree with the School of Information Science and Technology, Southwest Jiaotong University, Chengdu, China. From 2017 to 2019, he was a Visiting Ph.D. Student with the University of Victoria. He is also a Visiting Ph.D. Student with Guangzhou University, Guangzhou, China. His current research interests include buffer-aided communication, energy-harvesting wireless communication, and mobile edge computing.

Qingchun Chen (SM'14) received the B.Sc. degree and M.Sc. degree (Hons.) from Chongqing University, China, in 1994 and 1997, respectively, and the Ph.D. degree from Southwest Jiaotong University, China, in 2004. He was with Southwest Jiaotong University from 2004 to 2018. He is currently a Full Professor with Guangzhou University, Guangzhou, China. He has authored or coauthored over 100 research articles and two book chapters. He holds 40 patents. His research interests include wireless communication, wireless networks, information coding, and signal processing. He was a recipient of the 2016 IEEE GLOBECOM Best Paper Award. He has been serving as an Associate Editor for IEEE ACCESS since 2015.

Lin Cai (S'00–M'06–SM'10) received the M.A.Sc. and Ph.D. degrees (Hons.) in electrical and computer engineering from the University of Waterloo, Waterloo, Canada, in 2002 and 2005, respectively.

Since 2005, she has been with the Department of Electrical and Computer Engineering, University of Victoria, where she is currently a Professor. Her research interests span several areas in communications and networking, with a focus on network protocol and architecture design supporting emerging multimedia traffic and Internet of Things. She was a recipient of the NSERC E. W. R. Steacie Memorial Fellowships in 2019, the NSERC Discovery Accelerator Supplement (DAS) Grants in 2010 and 2015, and the Best Paper Awards of the IEEE ICC 2008 and the IEEE WCNC 2011. She has founded and chaired the IEEE Victoria Section Vehicular Technology and Communications Joint Societies Chapter. She has served as the TPC Symposium Co-Chair for the IEEE Globecom'10 and Globecom'13. She has been elected to serve the IEEE Vehicular Technology Society Board of Governors for the period 2019–2021. She has served as an Area Editor for the IEEE TRANSACTIONS ON VEHICULAR TECHNOLOGY, a member of the Steering Committee of the IEEE TRANSACTIONS ON BIG DATA (TBD) and the IEEE TRANSACTIONS ON CLOUD COMPUTING (TCC), an Associate Editor of the IEEE INTERNET OF THINGS JOURNAL, the IEEE TRANSACTIONS ON WIRELESS COMMUNICATIONS, the IEEE TRANSACTIONS ON VEHICULAR TECHNOLOGY, the IEEE TRANSACTIONS ON COMMUNICATIONS, the *EURASIP Journal on Wireless Communications and Networking*, the *International Journal of Sensor Networks*, and the *Journal of Communications and Networks* (JCN), and the Distinguished Lecturer of the IEEE VTS Society. She is also a Registered Professional Engineer of British Columbia, Canada.

Lisheng Fan received the bachelor's degree from the Department of Electronic Engineering, Fudan University, in 2002, the master's degree from the Department of Electronic Engineering, Tsinghua University, China, in 2005, and the Ph.D. degree from the Department of Communications and Integrated Systems, Tokyo Institute of Technology, Japan, in 2008. He is currently a Professor with Guangzhou University. He has published many articles in international journals, such as the IEEE TRANSACTIONS ON WIRELESS COMMUNICATIONS, the IEEE TRANSACTIONS ON COMMUNICATIONS, and the IEEE TRANSACTIONS ON INFORMATION THEORY, and in conferences, such as the IEEE ICC, the IEEE Globecom, and the IEEE WCNC. His research interests span in the areas of wireless cooperative communications, physical-layer secure communications, interference modeling, and system performance evaluation. He has also served as a member of the Technical Program Committees for the IEEE conferences, such as the IEEE Globecom, IEEE ICC, IEEE WCNC, and IEEE VTC. He has also served as the Chair of the Wireless Communications and Networking Symposium for Chinacom 2014. He is also a Guest Editor of the *EURASIP Journal on Wireless Communications and Networking*.